

# Crossing the streams: a framework for streaming analysis of short DNA sequencing reads

Qingpeng Zhang<sup>1</sup>, Sherine Awad<sup>2,3</sup>, C. Titus Brown<sup>2,1,3,\*</sup>

**1 Computer Science and Engineering,**

Michigan State University, East Lansing, MI, USA

**2 Microbiology and Molecular Genetics,**

Michigan State University, East Lansing, MI, USA

**3 Population Health and Reproduction,**

University of California, Davis, Davis, CA, USA

\* E-mail: [ctbrown@ucdavis.edu](mailto:ctbrown@ucdavis.edu)

March 9, 2015

## Abstract

We present a semi-streaming algorithm for k-mer spectral analysis of DNA sequencing reads, together with a derivative approach that is fully streaming. The approach can also be applied to genomic, transcriptomic, and metagenomic data sets. We develop two tools for short-read analysis based on these approaches, a method for semi-streaming k-mer-based error trimming, and a method for the analysis of error profiles in short reads using a streaming sublinear approach. These tools are implemented in the khmer software package, which is freely available under the BSD License at [github.com/ged-lab/khmer/](https://github.com/ged-lab/khmer/).

## 1 Introduction

K-mer spectral analysis is a powerful approach to error detection and correction in shotgun sequencing data that uses k-mer abundances to find likely errors in the data [1]. Approaches derived from spectral analysis can be very effective: spectral error correction achieves high accuracy, and Zhang et al. (2014) show that spectral k-mer trimming is considerably more effective at removing errors than quality score-based approaches [2, 3]. However, spectral analysis is also very compute intensive: most implementations count all the k-mers in sequencing data sets, which can be memory- or I/O-intensive for large data sets [3].

Streaming and semi-streaming algorithms can offer improved algorithmic and computational efficiency in the analysis of large data sets [4, 5]. Streaming algorithms typically examine the data only once, and have small, fixed memory usage. Semi-streaming algorithms may examine the

data a few times, with memory requirements that scale sublinearly with the size of the input data [6]. Streaming algorithms have not been applied to k-mer spectral analysis of sequencing reads, although Melsted et al. developed an effective streaming algorithm for calculating *aggregate* statistics of k-mer distributions from sequencing data [7], and the Lighter error corrector uses a low-memory semi-streaming multipass approach to do efficient error correction [8].

Brown et al. (2012) introduced a streaming algorithm for downsampling read data sets to normalize read coverage spectra, termed “digital normalization” (or “diginorm”) [9]. This procedure estimates the k-mer coverage of each read in a stream using an online algorithm. Reads above a certain estimated coverage are set aside and their k-mers are not tracked. The diginorm algorithm only examines the data once, and counts only the k-mers in retained reads, leading to sublinear memory usage for high-coverage data sets [9].

Here we develop a semi-streaming algorithm for k-mer spectral analysis, based on digital normalization, that can detect and remove errors in sequencing reads. This algorithm operates in sublinear memory with respect to the input data, and examines the data at most twice. The approach offers a general framework for streaming sequence analysis and could be used for error correction and variant calling. Moreover, the approach can be applied generically to data sets with variable sequencing coverage such as transcriptomes, metagenomes, and amplified genomic DNA. We also provide a fully streaming approach for estimating per-position sequencing error rates in reads that operates in fixed memory and only examines part of the input data.

## 2 Methods

The code used to generate all of the results in this paper is available at <http://github.com/ged-lab/2014-streaming/>; see README.md in that directory for instructions. The paper is completely reproducible from source data. The screed and khmer packages (screed v0.8 and khmer v1.4) were used to generate the results in this paper; both are freely available at <http://github.com/ged-lab/> under a BSD license.

### 2.1 Making synthetic data sets

We computationally constructed three small short-read DNA data sets for initial exploration of ideas. All synthetic sequences have equiprobable A/C/G/T. All synthetic reads are 100bp long and were sampled with 1% error. The “simple genome” data set consists of 1000 reads chosen uniformly from a 1 kb randomly constructed genome. The “simple transcriptome” data set consists of 568 reads chosen uniformly from synthetic transcripts containing different subsets of four 250-base exons, with expression levels varying by a factor of 30 from minimum to maximum. The “simple metagenome” data set consists of reads sampled from three different 500 bp sequences, across 30 fold variation in abundance. In all three

cases, the errors during read sampling were recorded for comparison with predictions.

## 2.2 Real data sets

We used three shotgun Illumina data sets: a genomic data set from *E. coli*, a mRNAseq data set from *Mus musculus*, and a mock community metagenome. For *E. coli*, we took a 5m read subset of ERA000206 from [10]. For mRNAseq, we used a 10m read subset of GSE29209 from [11]. For the mock metagenome, we used a 20m read subset of SRR606249 from [12]. Prior to analysis, we eliminated any read with an 'N' in it and filtered the reads by mapping to the known references, yielding the read numbers in Table 1.

## 2.3 K-mer cardinality statistics

K-mer counts in Table 5 were calculated using the HyperLogLog cardinality counting algorithm [13]. The implementation used is implemented in khmer, script `sandbox/unique-kmers.py`, using the default error rate of 0.01.

## 2.4 K-mer spectral analysis

All spectral error analysis was done by finding the beginning and end point of runs of low-abundance k-mers in each read. For normalized data, we used a low-abundance cutoff of 3; for non-normalized data, we used a low-abundance cutoff of 10. These cutoffs were chosen by examining the k-mer abundance plot (Figure 1).

Spectral error analysis was implemented in the khmer module Python function `find_spectral_error_positions`. We used `report-errors-by-read.py` to predict errors on normalized data, and `calc-errors-few-pass.py` to do semi-streaming error analysis; both scripts are in `2014-streaming/pipeline/`. Variable coverage error analysis was enabled with the `-V` parameter to both scripts.

## 2.5 Digital normalization

We ran digital normalization on all data sets using khmer's `normalize-by-median.py` script, with a k-mer size of 20 and a target coverage of 20; these parameters have been shown to yield good performance for assembly prefiltering [9, 14]. khmer relies on a memory efficient Count-Min Sketch data structure that yields occasional inaccurate counts; memory parameters were chosen for each data set so that the false positive rate was under 1%, below which it has no significant effect on outcomes [3].

## 2.6 Read mapping and error correction

We used Quake v0.3.5, Jellyfish 1.1.11, Boost 1.57.0, and bowtie2 v2.1.0 to generate results [2, 15, 16, 17]. `bowtie2` was run with default parameters.

Quake’s `count-qmers` was used to generate a k-mer count with `-q 33 -k 14`, and `correct` was also run with `-q 33 -k 14`. The correction threshold (`-c`) was chosen automatically by Quake as per the manual, and was 7.94 for *E. coli* diginorm, 7.2 for *E. coli* original, and 6.26 for the high-coverage mRNAseq sample.

## 2.7 Semi-streaming error analysis and trimming

We used the script `calc-errors-few-pass.py` to do semi-streaming error analysis; it is available in the `2014-streaming` repository. We used a normalization coverage threshold of 20 and a trusted k-mer cutoff of 3.

The khmer script `trim-low-abund.py` was used for semi-streaming error trimming, with the same parameters as above. The khmer script `calc-error-profile.py` was used for sublinear time and space error analysis with default parameters. The pipeline script `report-errhist-2pass.py` was used for comparison purposes.

The `calc-error-profile.py` script iterates through the read data set, loading low-coverage reads into the graph and analyzing the error positions in high-coverage reads using the spectral error location function as above. The script exits when any one of three conditions is met: (1) in the most recent sample of 25,000 reads, more reads have been profiled than loaded into the graph; (2) more than 20,000 reads total have profiled; or (3) more than 100m reads have been loaded. The second condition was satisfied for both data sets analyzed in this work.

## 3 Results

### 3.1 Coverage-normalized data can be used to locate and correct errors in high-coverage shotgun sequencing data

Digital normalization eliminates many erroneous k-mers, while retaining the majority of true k-mers [9]. Our initial question was whether we could apply spectral error analysis to genomic short read data using counts from digitally normalized data. This would allow us to take advantage of the space savings of digital normalization when storing and examining k-mer counts. We tested this on a synthetic data set and an *E. coli* data set. We then compared the performance of the Quake genomic error counter on the original and digitally normalized counts from the *E. coli* data [2].

**Simulated data:** We first applied digital normalization to a simulated data set with known errors. We generated the synthetic data set from a simulated low-complexity genome (“simple genome”; see Methods for generation and Table 1 for data set details). We then applied digital normalization to these synthetic reads, normalizing to a median 20-mer coverage of 20 ( $k=20$ ,  $C=20$ ).

The k-mer spectrum before and after digital normalization is shown in Figure 1. While the total number of k-mers decreased in the digitally normalized data set, the separation between the high count k-mers

Name	Number of reads	Description
simple genome	1000	1kb genome; no repeats
<i>E. coli</i> MG1655	4,863,836	Subset of ERA000206 ([10])
simple transcriptome	568	300:1 high:low abundance; shared exons
mouse mRNAseq	7,915,339	Subset of GSE29209 ([11])
simple metagenome	2,347	316:1 high:low abundance species
mock metagenome	18,805,251	Subset of SRR606249 ([12])

Table 1: **Data sets used for evaluation.**

and the low-count k-mers remains clear. The key concept underlying k-mer spectral error analysis is that in a high-coverage data set, these high count k-mers will represent *correct* k-mers, while the low count k-mers are produced by errors in the reads. Simple classification methods suffice to identify and trim or correct these low-count k-mers.

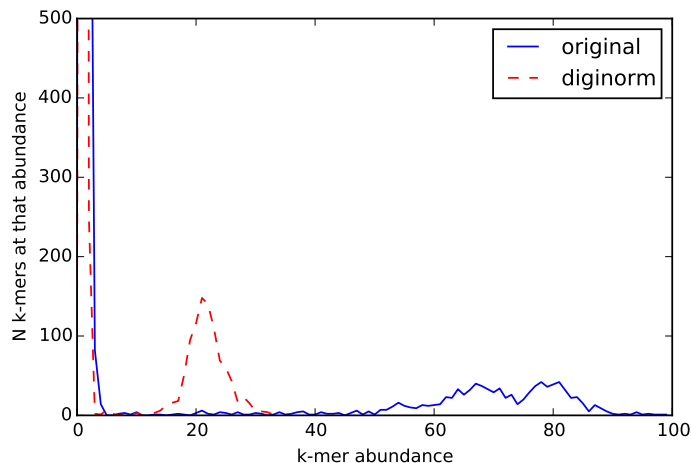


Figure 1: **K-mer spectrum of a simple artificial data set, before and after digital normalization.** The peaks at the origin represents erroneous k-mers resulting from (simulated) error; the peaks centered at 80 (original) and 20 (diginorm) represent k-mers truly present in the genome, which are shared among many reads.

We next used k-mer counts from the downsampled read set to detect errors in the original read set. The algorithm is straightforward: we look for bases at the beginning or ends of low-abundance runs of k-mers in each read, which should signify the locations of errors. We used a “trusted k-mer” cutoff of  $C_0 = 3$  as our abundance cutoff, below which we assumed k-mers were erroneous (see Methods). The results are presented in Table 2. Of the 633 simulated reads from the simple genome that contain one or more errors, predicted errors matched the known truth exactly for 485 of

Simple genome	Original counts	Diginorm counts
Perfect detection (TP)	474	485
No errors (TN)	355	366
Miscalled errors (FP)	159	148
Mispredicted errors (FP)	12	1
Missed errors (FN)	0	0
Sensitivity	100%	100%
Specificity	67.5%	71.1%

Table 2: **Results from spectral error detection on 1000 synthetic reads from a simulated 10kb genome, using k-mer counts from original or digitally normalized reads. The counts in the table are the number of reads where all errors were detected perfectly (TP), errors were present and none were called (TN), one or more errors were miscalled (one type of FP), errors were mistakenly called in an error-free read (the other type of FP), and errors present in a read were missed (FN).**

them (true positives), and 366 reads were correctly predicted to contain no errors (true negatives). 0 reads were falsely predicted to have no errors (false negatives). The errors in 148 reads were miscalled – while the reads each had one or more errors, the positions were not correctly called – and one read was incorrectly predicted to contain errors, leading to a total of 149 false positives. From this, we calculated the prediction sensitivity to be 100% and the prediction specificity to be 71.1%.

When we applied spectral error detection using the counts from the original (un-normalized) reads, we saw similar results: 474 TP, 355 TN, 171 FP, and 0 FN, for a sensitivity of 100% and a specificity of 67.5% (Table 2). (Note: for this analysis we used a cutoff of  $C_0 = 10$ .)

***E. coli* reads:** We next applied digital normalization and k-mer spectral error detection to an Illumina data set from *E. coli* MG1655 [18]. In real reads, we do not know the location of errors; to calculate likely errors, we mapped 4.9m untrimmed reads to the known *E. coli* MG1655 genome with bowtie2 [17] and recorded mismatches between the reads and the genome. These mismatches were taken to be errors in the reads. We found 8.0m errors in 2.2m reads, for an overall error rate of 1.60%.

We then compared the results of k-mer spectral error detection with and without digital normalization. We used the same parameters as on the simulated genome ( $C_0 = 10$  for unnormalized,  $C_0 = 3$  for normalized). The results are presented in Table 3. Using the original counts, the sensitivities were close to the predictions from the normalized counts: using the original counts, we achieved a sensitivity of 99.7%, versus 99.2% using the counts from the digitally normalized reads. The specificities were also comparable – 68.8% using the original counts, and 68.7% using the digitally normalized counts.

<b>E. coli</b>	Original counts	Diginorm counts
Distinct k-mers	39,677,503	26,510,104 (67%)
Perfect detection (TP)	819,233	808,657
No errors (TN)	2,782,265	2,782,403
Miscalled errors (FP)	1,082,566	1,088,787
Mispredicted errors (FP)	177,637	177,499
Missed errors (FN)	2,135	6,490
Sensitivity	99.7%	99.2%
Specificity	68.8%	68.7%

Table 3: **Results from spectral error detection on 4.9m *E. coli* reads, using k-mer counts from original (left column) and digitally normalized (right column) reads.**

	original	diginorm
Total reads, after Quake	4,805,561	4,804,947
Erroneous reads discarded	58,275	58,889
Total bp	441,752,819	441,701,309
Total errors remaining	47,510	41,455
Per-base error rate	0.011%	0.009%

Table 4: **Comparison of Quake results when run on the same *E. coli* data set, using k-mer counts from either the original data set (original) or the digitally normalized reads (diginorm). All numbers are post-error correction; the original error rate was 1.60%.**

Sample	original unique k-mer count	normalized unique k-mer count
<i>E. coli</i>	39,677,503	26,510,104 (67.8%)
mouse mRNAseq	54,177,799	48,058,631 (88.7%)
mock metagenome	201,459,416	201,093,236 (99.8%)

Table 5: **Unique k-mer counts for original and normalized data sets using a k-mer size of 20 and the specified coverage cutoff. Digital normalization reduces the total number of k-mers in the data set for high coverage data sets.**

Sample	original read count	normalized read count
<i>E. coli</i>	4,863,836	1,609,639 (33.1%)
Mouse RNAseq	7,915,339	3,832,453 (48.4%)
Mock metagenome	18,805,251	17,353,291 (92.2%)

Table 6: **Read counts for original and normalized data sets using a k-mer size of 20 and the specified coverage cutoff. Digital normalization reduces the total number of reads for later analyses.**

***E. coli* error correction with Quake:** While the results above suggest that simple spectral error detection works equally well both before and after digital normalization, we were concerned that we might lose informative reads and k-mers during digital normalization. To evaluate this, we used Quake [2] to perform error correction on the data set using the k-mer counts from the digitally normalized reads, and compared the results to error correction with the entire read data set.

The results of running Quake on the original data using counts from the original and digitally normalized data are shown in Table 4. The performance was essentially the same: Quake brought the overall error rate in the data set from 1.60% (8.0m errors) to 0.01% (40,000 errors).

These results demonstrate that digitally normalized counts retain all of the information necessary for effective error correction with Quake, despite there being many fewer k-mers (Table 5) and far fewer reads (Table 6) being used as input into the k-mer count table.

### 3.2 Coverage-normalized data can be used to locate errors in variable coverage shotgun sequencing data

One of the drawbacks of spectral abundance analysis is that it does not directly apply to data with variable coverage. For example, metagenomic or transcriptomic data sets typically contain reads from both high-abundance and low-abundance molecules. This in turn leads to high coverage and low coverage reads in the same data set. This variability in coverage confounds naive spectral analysis for two reasons: first, erroneous k-mers from very high abundance regions can accumulate and increase in abundance over the threshold for trusted k-mers, thus appearing to be correct (the so-called “curse of deep sequencing” [19]); and second, correct reads from low coverage regions yield k-mers below the trusted k-mer threshold that appear to be incorrect. In practice, therefore, error analysis for metagenomic and transcriptome data uses other approaches than direct spectral error analysis [20, 21, 22].

Digital normalization works on genomic data, with even coverage, as well as on variable coverage data such as transcriptome and metagenome data [9, 14, 23]. Using the reference-free estimator of per-read coverage developed for digital normalization, the median k-mer abundance within a read, we developed a general approach that enables spectral error analysis on variable coverage data. We then applied this to two synthetic data sets as well as two real data sets, a mock shotgun metagenome and mRNAseq data from mouse.

**Coverage-normalized spectral error analysis:** Using digital normalization, we should be able to address both the problem of *too high* coverage and *too low* coverage. First, by applying digital normalization to variable coverage data and then working only with the k-mer counts from the normalized reads, we can avoid counting high abundance errors as correct. Second, by ignoring reads with a low estimated coverage, we can



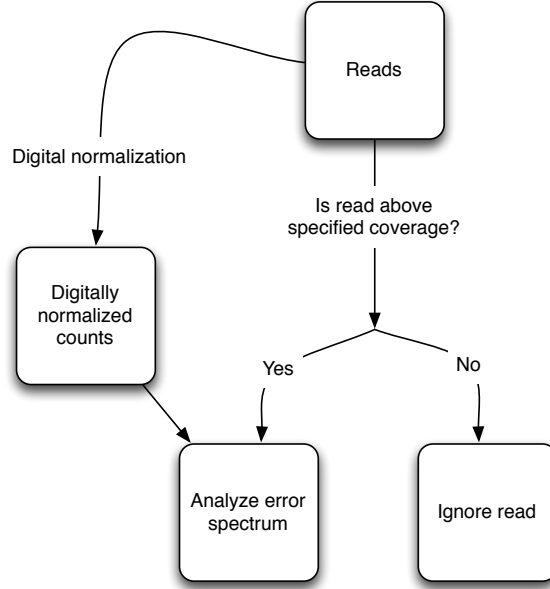


Figure 2: Coverage-normalized spectral error analysis. Reads are normalized, and high-coverage reads are subjected to spectral error analysis with the normalized counts, while low-coverage reads are ignored.

avoid misclassifying true low-abundance k-mers as errors. The process is shown in Figure 2.

**Simulated data:** To test this approach, we generated two more synthetic data sets, “simple metagenome” and “simple mRNAseq,” which contain both high- and low-abundance species (see Table 1 for data set details). After generating synthetic reads with a 1% error rate and applying digital normalization ( $k=20/C=20$ ), we again used the normalized counts to do spectral error detection. However, we used a modified algorithm that only examined reads with a median k-mer abundance of  $C$  or greater.

The results of running error detection on the synthetic metagenome and mRNAseq data sets are shown in Table 7.

For the simple mRNAseq data set, 524 of 568 reads (92.3%) met the coverage criterion. Of the 524 reads analyzed, the errors in 228 erroneous reads were called perfectly (TP) and 235 of the reads with no errors were correctly called as error-free (TN). No reads were incorrectly determined to be error-free (FN). Of the remaining 61 errors, 52 were miscalled (reads with errors were called correctly but the locations were not correctly determined) and 9 reads were incorrectly called as erroneous when they were in fact correct. We calculated the prediction sensitivity to be 100% and the prediction specificity to be 79.4%. For the simple metagenome data set,

	simple mRNAseq	simple metagenome
Total reads	568	2347
High coverage reads	524 (92.3%)	2254 (96.0%)
Perfect detection (TP)	228	978
No errors (TN)	235	1098
Miscalled errors (FP)	52	170
Mispredicted errors (FP)	9	6
Missed errors (FN)	0	2
Sensitivity	100%	99.8%
Specificity	79.4%	86.2%

Table 7: **Variable coverage spectral error detection on two synthetic data sets, a simple mRNAseq data set and a simple metagenome. Per-read coverage was estimated by median k-mer abundance within the read, and only the reads with estimated coverage at or above the specified threshold were analyzed. Digitally normalized counts were used for the spectral error analysis.**

2254 of 2347 reads (96.0%) met the coverage criterion, with 978 TP, 1098 TN, 2 FN, and 176 FP, for a prediction sensitivity of 99.8% and a prediction specificity of 86.2%. (In neither case did we include low-coverage reads in the statistics.)

Importantly, these results are roughly comparable to the results on the synthetic genome (100.0% sensitivity and 71.1% specificity with the same parameters; see Table 2).

**mRNAseq data:** To evaluate coverage-normalized spectral analysis on real data, we applied variable coverage spectral error analysis to 7.9m mouse mRNAseq reads [24]. After calling errors in the reads by mapping them back to the known genomes, we used spectral analysis to identify putative errors. The results are shown in Table 8, second column. We achieved 80.4% sensitivity and 88.7% specificity on the 5.4m high coverage reads in this data set.

**Mock metagenome data:** We next applied our approach to 18.8m reads from a diverse mock community data set [12]. We found 4,954,341 reads were at or above this coverage threshold. Here errors were again calculated by mapping the reads to the known reference and finding mismatches. The results are shown in Table 8, third column. We achieve 87.1% sensitivity and 98.0% specificity on the high coverage reads.

**Error correcting variable coverage data with Quake:** There are many sophisticated error correction algorithms implemented for shotgun genome data, but relatively few work directly on variable coverage data such as mRNAseq [20, 21]. Digital normalization, in theory, could enable the use of *any* spectral error correction algorithm on the high coverage components of data sets.

	mouse mRNAseq	mock metagenome
Total reads	7,915,339	18,805,251
High coverage reads	5,379,738 (68.0%)	4,954,341 (26.4%)
Perfect detection (TP)	1,099,492	115,925
No errors (TN)	3,560,733	4,723,053
Miscalled errors (FP)	429,842	54,041
Mispredicted errors (FP)	22,384	44,178
Missed errors (FN)	267,287	17,144
Sensitivity	80.4%	87.1%
Specificity	88.7%	98.0%

Table 8: **The results of variable coverage spectral error detection on two real variable coverage data sets, a mouse mRNAseq data set and a mock shotgun metagenome. Per-read coverage was estimated by median k-mer abundance within the read, and only the reads with estimated coverage at or above the specified threshold were analyzed. Digitally normalized counts were used for the spectral error analysis.**

mRNAseq	diginorm
Total reads	7,915,339
High coverage reads	5,379,738
Erroneous reads discarded	509,979
Total bp after correction	348,994,329
Total errors remaining	1,469,618
Per-base error rate	0.42%

Table 9: **Results of running Quake on high-coverage reads from mouse mRNAseq, using k-mer counts from the digitally normalized reads. The original error rate was 1.0%.**

288 To evaluate this, we again used Quake (a genomic error corrector)  
289 to correct the high coverage mRNAseq reads using the diginorm counts.  
290 We first extracted the 5.4m reads with estimated coverage greater than  
291 or equal to 20 from the mouse mRNAseq data set, and then digitally  
292 normalized the data. We next applied the Quake error corrector to the  
293 unnormalized high-coverage reads using the k-mer counts from the nor-  
294 malized reads, as with the *E. coli* data set. Quake discarded 510,000 reads  
295 and corrected the remainder, bringing the error rate from 1.0% to 0.42%  
296 - see Table 9. As with *E. coli*, this suggests that sufficient information  
297 remains in the digitally normalized data to do an effective job of error  
298 correction.

### 3.3 A semi-streaming algorithm can be used for spectral error analysis

The spectral error detection approach outlined above is a 2-pass offline algorithm for any given data set - the first pass normalizes the read set and records the k-mer abundances, while the second pass analyzes the reads for low-abundance k-mers. Even with digital normalization reducing the number of k-mers under consideration, this 2-pass approach is time consuming on large data sets. Below, we develop an approach that considers many of the reads only once.

**Semi-streaming analysis of coverage-saturated regions:** Shotgun sequencing oversamples most regions – for example, for a 100x coverage genomic data set, we would expect 50% or more of the genome to be represented by more than 100 reads. This is a consequence of the Poisson-random sampling that underlies shotgun sequencing [25]. This oversampling provides an opportunity, however: if we regard the read data set as a stream of incoming data randomly sampled from a pool of molecules, high-abundance species or subsequences within the pool will be more highly sampled in the stream than others, and will thus generally appear earlier in the stream. For example, in mRNAseq, highly expressed transcripts should almost always be sampled much more frequently than low-expressed transcripts, and so more reads from highly expressed transcripts will be seen in any given subset.

With this in mind, we can adapt the same approaches used in previous sections to do *semi-streaming* error analysis by detecting and analyzing high-coverage reads *during* the first pass. Here we again use the median k-mer abundance of the k-mers in a read to estimate that read’s abundance [9]; crucially, this can be done at any point in a stream, by using the online k-mer counting functionality of khmer to determine the abundance of k-mers seen thus far in the stream [3].

The conceptual idea is presented in Figure 3. On the first pass, low-coverage reads would be incorporated into the k-mer database and set aside for later analysis, while high-coverage reads would be analyzed for errors. On the second pass, the set aside reads would be checked for coverage again, and either ignored or analyzed for errors. Crucially, this second pass involves *at most* another full pass across the data, but only when the entire data set is below the coverage threshold; the larger the high coverage component of the data, the smaller the fraction of the data that is examined twice.

In Figure 4, we show diginorm-generated coverage saturation curves for both real and error-free simulated reads from *E. coli* MG1655. In both cases, after the first 1m reads, the majority of reads have an estimated coverage of 20 or higher, and hence can be used for error analysis on the remainder of the data encountered in the first pass.

Moreover, because only the normalized counts are used in spectral analysis, the approach should apply equally well to data sets with uneven coverage, i.e. metagenomes and transcriptomes. To test this, we first apply this semi-streaming error detection approach to the three synthetic data sets used earlier, and then to the three real data sets.

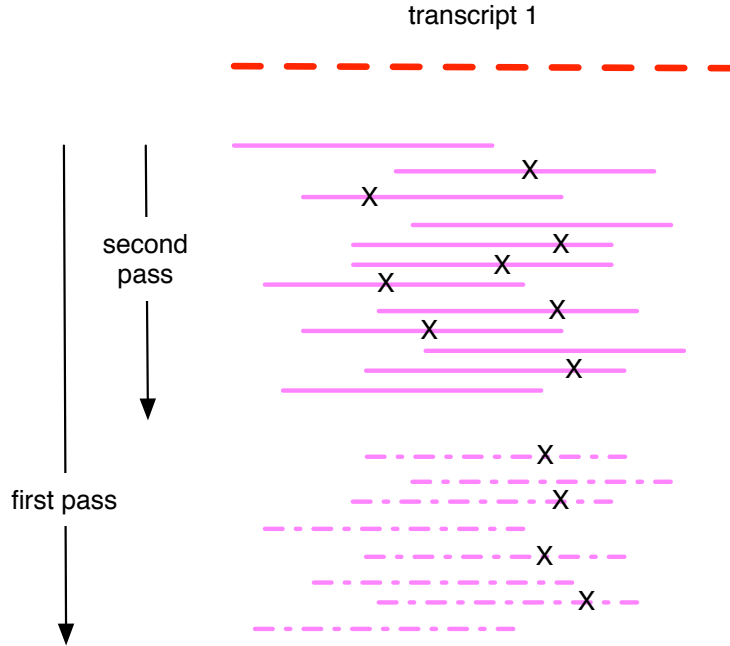


Figure 3: **Diagram of semi-streaming error detection.** In a first pass over the read data, reads are loaded in until the graph locus to which they belong is saturated. From that point on, reads are examined for errors and not loaded into the graph. In a second pass, only the subset of reads loaded into the graph are examined for errors.

**Streaming error analysis of synthetic data:** Using the semi-streaming approach on the “simple genome” reads, we obtain nearly identical numbers to the full two-pass approach: 485 TP, 365 TN, 150 FP, and 0 FN, for a sensitivity of 100% and a specificity of 70.9% (Table 10). However, with the semi-streaming algorithm, only 320 of the 1000 reads are examined twice. Likewise, for the “simple mRNAseq” and “simple metagenome” data sets, we obtain identical and nearly identical results, respectively; due to differences in the order in which reads are examined, the simple metagenome fails to detect one true positive and erroneously finds errors in three extra reads. On the mRNAseq data set, 33.1% of the reads are examined twice, and on the metagenome, 380 of 2347 (16.2%) of the reads are examined twice.

**Semi-streaming error analysis of real data:** We also get similar quality results on the real data sets when comparing two-pass error detection with semi-streaming error detection (Table 11). For *E. coli*, with semi-streaming error detection we obtain a sensitivity of 99.4% and a specificity of 68.7%, compared to 99.2% and 68.7% with the two-pass approach (Table 3). For the mRNAseq data set, we see a sensitivity of

	simple genome	simple mRNAseq	simple metagenome
Number of passes	1.32	1.16	1.33
Perfect detection (TP)	485	228	977 (-1)
No errors (TN)	365 (-1)	235	1095 (-3)
Miscalled errors (FP)	148	52	171 (+1)
Mispredicted errors (FP)	2 (+1)	9	9 (+3)
Missed errors (FN)	0	0	2
Sensitivity	100.0%	100.0%	99.8%
Specificity	70.9%	79.4%	85.9%

Table 10: **Results from applying semi-streaming error detection to the same synthetic data sets as in Table 2 and Table 7.** Number of passes is the average number of times each read in the data set was examined; numbers in parentheses give the difference between these numbers and the previous results.

	<i>E. coli</i>	mouse mRNAseq	mock metagenome
Number of passes	1.33	1.48	1.92
Perfect detection (TP)	810,896	1,162,662 (+61,370)	116,833
No errors (TN)	2,781,961	3,552,261	4,717,494
Miscalled errors (FP)	1,087,775	418,481	53,349 (-692)
Mispredicted errors (FP)	177,914	30,856 (+8472)	49,737 (+5559)
Missed errors (FN)	5263 (-1227)	215,478 (-51,809)	16,928
Sensitivity	99.4%	84.4% (+4.0%)	87.3%
Specificity	68.7%	88.8%	97.9%

Table 11: **Results from applying semi-streaming error detection to the same real data sets as in Table 3 and Table 8.** Number of passes is the average number of times each read in the data set was examined; unless noted in parentheses, numbers were within 1% of non-streaming results.

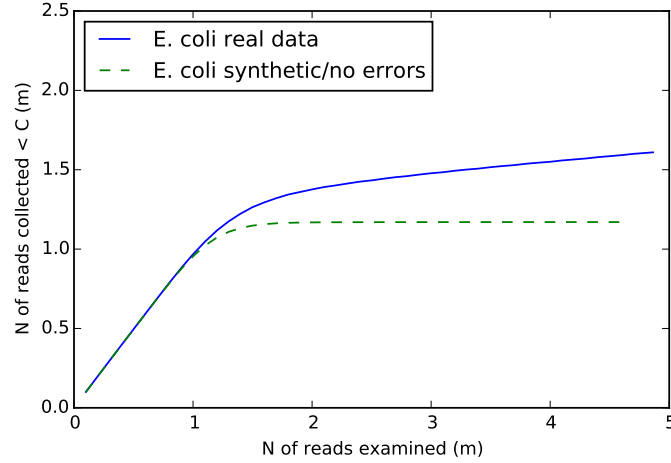


Figure 4: **Saturation curve of a real and a simulated *E. coli* read data set.** Reads are collected when they have an estimated coverage of less than 20; in the early phase (< 1m reads), almost all reads are collected, but by 2m reads into the data set, the majority of reads come from loci with an estimated sequencing depth of > 20 and are rejected.

365 84.4% with semi-streaming vs 80.4% with two-pass, and a specificity of  
 366 88.8% vs 88.7% for semi-streaming vs two-pass, respectively. And for the  
 367 mock metagenome, we have a sensitivity of 87.3% with semi-streaming,  
 368 vs 87.1% with the two-pass approach; and a specificity of 97.9% for semi-  
 369 streaming and 98.0% two-pass (compare Table 11 and Table 8). However,  
 370 the semi-streaming approach examined the *E. coli* data only 1.33 times,  
 371 the mRNAseq data 1.48 times, and the metagenome data 1.92 times on  
 372 average.

### 373 3.4 A semi-streaming algorithm can be used for 374 error trimming

375 Once errors can be *detected* with a semi-streaming algorithm, errors can  
 376 also be *removed* by trimming reads at the first base predicted to be erro-  
 377 neous in a read. This approach is remarkably effective, but can require  
 378 considerably more memory than quality-score based trimming [3]. More-  
 379 over, it is generally implemented as an offline (two-pass) algorithm. Be-  
 380 low, we apply the same semi-streaming approach shown in Figure 3 to  
 381 trimming reads.

382 **Semi-streaming error trimming on synthetic data:** On the  
 383 “simple genome” with counts from the digitally normalized reads, this

trimming approach eliminates 149 reads entirely and truncates another 392 reads. Of the 100,000 bp in the simulated reads, 31,910 (31.9%) were removed by the trimming process. In exchange, trimming eliminated *all* of the errors, bringing the overall error rate from 0.63% to 0.00%.

For the simple metagenome we used the variable abundance approach described above and only trimmed reads with estimated coverage of 20 or higher. Here, of 2347 reads containing 234,700 bp, 314 reads (13.4%) were removed and 851 reads (36.3%) were trimmed, discarding a total of 74,321 bases (31.7%). Of 1451 errors total, all but 61 were eliminated, bringing the overall per-base error rate from 0.62% to 0.04%. The simple mRNAseq data set showed similar improvement: 83 of 568 reads were removed, and 208 were trimmed, removing 19,507 of 56,800 bases (34.34%). The initial error rate was 0.65% and the final error rate was 0.07%.

**Semi-streaming error trimming on real data:** Applying the semi-streaming error trimming to the *E. coli* MG1655 data set, we trimmed 2.0m reads and removed 50,281 reads entirely. Of 8.0m errors, all but 203,345 were removed, bringing the error rate from 1.49% to 0.07%. Trimming discarded 53 Mbp of the original 486 Mbp (11.1%).

On the mouse mRNAseq data set, semi-streaming error trimming removed 919,327 reads and trimmed 648,322 reads, removing 19.8% of the total bases, bringing the overall error rate from 1.59% to 1.21%. When we measured only the error rate in the high-coverage reads, trimming brought the error rate from 1.20% to 0.42%. On the mock metagenome data set, 27,554 reads were removed and 171,705 reads were trimmed, removing 0.36% of bases; this low percentage is because of the very low coverage of most of the reads in this data set.

### 3.5 Illumina error rates and error profiles can be determined from a small sample of sequencing data

With Illumina sequencing, average and per-position error rates may vary between sequencing runs, but are typically systematic within a run [26]. Melsted and Halldorson (2014) introduced an efficient streaming approach to estimating per-run sequencing error, but this approach does not apply to error rates by position within reads [7]. Here, k-mer spectral error analysis can be used to calculate per-position relative sequencing error for entire data sets [3].

We can adapt the streaming approaches above to efficiently provide estimates for *subsets* of the data. The basic idea is to consume reads until some reads have saturated, and then to calculate error rates for new reads from the saturated loci in the graph. This can be done in one pass for data sets with sufficiently high coverage data: as shown above (Figure 4), in some data sets, most of the reads will have sufficient coverage to call errors by the time 20% of the data set has been consumed.

Using the same error detection code as above, we implemented a sub-linear memory/sublinear time algorithm that collects reads until some regions have reached 20x coverage, or 200,000 reads have surpassed a coverage of 10x (see Methods for details). In either case, all reads at or above



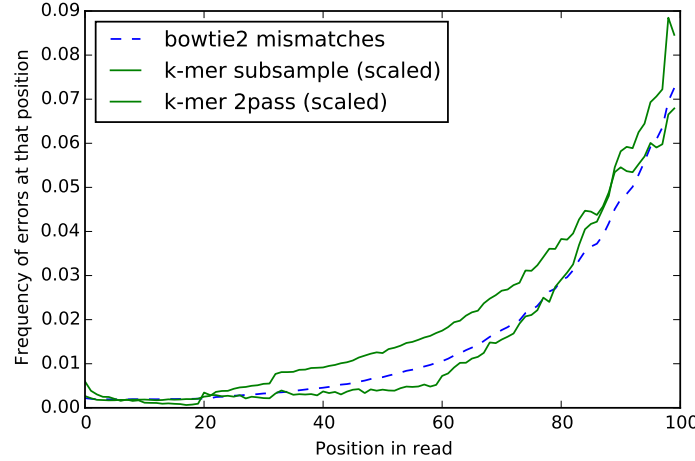


Figure 5: **Error spectrum of reads in the *E. coli* data set.** The sublinear k-mer spectrum analysis is calculated based on saturation of a fraction of the data set, while the two-pass spectral analysis uses all of the data. bowtie2 mismatches are based on all mapped reads. The y values for the k-mer spectral analyses are scaled by a factor of four for ease of comparison.

a coverage of 10 are analyzed for errors, with a trusted k-mer cutoff of 3. In Figure 5 and Figure 6 we show the resulting error profiles for the *E. coli* and mouse RNAseq data sets, compared with the profile obtained by examining the locations of mismatches to the references. We also show the error profile obtained with the full two-pass approach (using digital normalization and then error detection as above) for comparison.

In the *E. coli* data set (Figure 5), we see the increase in error rate towards the 3' end of the gene that is characteristic of Illumina sequencing [27]. All three error profiles agree in shape (Pearson's correlation of 0.99 between each pair) although they are offset considerably in absolute magnitude. The k-mer error profile was calculated from the first 850,000 reads, but is consistent across five other subsets of the data chosen randomly with reservoir sampling (data not shown); all five subsets had Pearson's correlation coefficients greater than 0.99 with the bowtie2 mapping profile and the two-pass spectral approach.

The RNAseq error profile exhibits two large spikes, one at position 34 and one at position 69. Both spikes appear to be genuine and correlate with large numbers of Ns in those positions in the original data set. The spikes are present in the profiles derived from two-pass spectral analysis as well as the bowtie2 mismatch calculation. However, the sublinear approach does not detect them when using the first 675,000 reads. This is because of the choice of subsample: five other subsamples, chosen randomly from the entire data set with reservoir sampling, match the

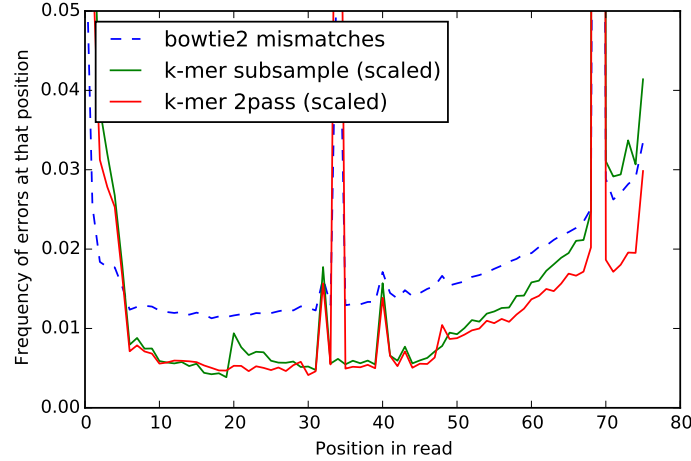


Figure 6: **Error spectrum of reads in the mouse RNAseq data set.** The sublinear k-mer spectrum analysis is calculated based on saturation of a fraction of the data set, while the two-pass spectral analysis uses all of the data, and bowtie2 mismatches are based on all mapped reads. The peak of errors at position 34 in the bowtie2 mapping reflects errors that in the first part of the data set are called as Ns, and hence are ignored by the sublinear error analysis; see text for details. Note, the bowtie2 mismatch rates are larger than the spectral rates, so for ease of comparison the y values for the k-mer spectral analyses are scaled by a factor of four.

match the two-pass spectral analysis (data not shown). The error profiles calculated from all six subsamples with the sublinear algorithm have a Pearson's correlation coefficient greater than 0.96 with the error profiles from the full two-pass spectral approach and the bowtie2 mismatches.

### 3.6 Performance on full mRNAseq and metagenomic data sets

In practice, the space and time performance of both digital normalization and the generalized streaming approach presented here depend on specific details of the data set under analysis and the precise implementation of the coverage estimator. While our intention in this paper is to demonstrate the general streaming approach, we note that even our naive implementation for e.g. streaming trimming is useful and can be applied to very large data sets. For high coverage data, we can efficiently error-trim 10s of millions of reads in both sublinear memory and fewer than two passes across the data. In Table 13, we show the summary statistics for streaming error trimming of the full mouse mRNAseq and mock

Data set	pre-trim error	% bp trim	% reads trim	post-trim error
<i>E. coli</i>	1.49%	11.05%	41.9%	0.07%
mouse mRNAseq	1.59%	13.9%	19.8%	1.21%
(high coverage only)	1.20%	20.4%	29.0%	0.42%
Mock metagenome	0.31%	0.4%	1.1%	0.28%
(high coverage only)	0.16%	1.4%	3.5%	0.07%

Table 12: **A summary of trimming statistics for semi-streaming error trimming. Error rates before and after trimming were estimated by mapping. “High coverage” numbers refer to the subset of reads with  $C \geq 20$  that were subject to analysis.**

Data set	mouse mRNAseq	mock metagenome
Total reads	81.3m	103.2m
Total bp	6.18 Gbp	10.4 Gbp
High-coverage reads	74.6m	91.9m
Number of passes	1.18	1.43
% reads trim	25.0%	11.75%
% bp trim	13.74%	4.03%
Pre-trim error rate	1.89%	0.27%
Post-trim error rate	1.30%	0.15%

Table 13: **Results of streaming error trimming on complete data sets. Error rates before and after trimming were estimated by mapping.**

metagenome data; in contrast to the smaller subsets used previously (see Table 12), when we consider the full data sets the majority of reads are examined only once (see “Number of passes”, Table 13).

### 3.7 Time and space considerations

Shotgun DNA sequencing gives us a stream of items representing sentences (“reads”) randomly sampled from a larger text, with replacement. In this paper, our primary goal is to efficiently identify the locations of errors in these reads by finding differences with respect to the (unknown) source text; however, this problem is a gateway to a larger set of interesting domain problems, which includes estimating the true abundance of the sentences in the larger text and determining the complete composition of the source text.

There are several distinct features of this problem that bear mentioning. The first is that important details of the source text, such as its size and statistical composition, may be completely unknown; that is, often the reads themselves are the most specific information we have about the source text. Second, the source text may be incompletely sampled by the reads, and whether or not it is completely sampled may not be known in advance. And third, read data sets are typically stored on disk, at least in current implementations; our goal is to identify more efficient approaches

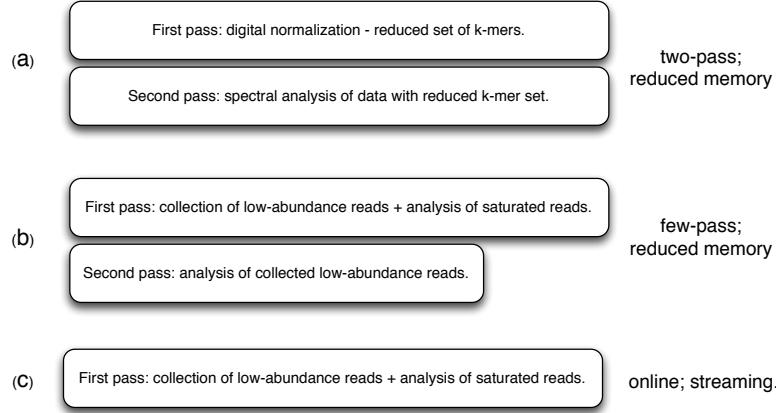


Figure 7: **A summary of the three approaches to k-mer spectral analysis presented above. (a) Digital normalization reduces the set of k-mers to be used for the second pass analysis of the full data set. (b) Combining online saturation analysis with collection of reads yields a few-pass algorithm. (c) When all of the data does not need to be analyzed, online detection of saturation can be used to drive the analysis of saturated portions of the reads and graph.**

to examining these data sets without necessarily moving to a pure streaming model, which allows us to make use of the *semi-streaming* paradigm introduced by Feigenbaum et al. [6].

We address this problem by making use of k-mer spectra, a common approach in which reads are treated as subpaths through a De Bruijn graph, and errors in the reads are identified by finding low-frequency subpaths [1]. We generalize this approach by building the graph with an online algorithm and detecting regions of the graph saturated by observations. These regions can then be used for per-read analysis without necessarily examining the entire data set.

**Detecting graph saturation:** We detect graph saturation with digital normalization. The digital normalization algorithm is, in Python pseudocode:

```
for read in data:
    if coverage(read, table) < DESIRED:
        add_read_to_graph(read, graph)
        analyze(read)
```

This is a single-pass algorithm that can be implemented in fixed space using a Count-Min Sketch to store the De Bruijn graph necessary for coverage estimation [28, 3]. For any error-containing data set with coverage greater than `DESIRED`, the graph requires space less than the size of the input - typically space sublinear in the data size, for any fixed-size source text (see Figure 4 and [3]).

512 The digital normalization algorithm was developed as a *filter*, in which  
 513 the reads are passed on to another program (such as a *de novo* assembler)  
 514 for further analysis – these later analyses are typically based on multi-pass,  
 515 heavyweight algorithms. Here, digital normalization is performing lossy  
 516 compression, reducing the number of error-containing sentences while at-  
 517 tempting to retain the structure of the De Bruijn graph [9, 3, 14]. This  
 518 reliance on a post-normalization heavyweight analysis step limits the ap-  
 519 plicability of digital normalization and presents challenges in the analysis  
 520 of extremely large data sets, which motivated this work.

521 **Semi-streaming analysis:** The algorithm for *semi-streaming* analy-  
 522 sis of reads is as follows:

```
523 for read in data: # first pass
524     if coverage(read, graph) < DESIRED:
525         add_read_to_graph(read, graph)
526         save(read)
527     else:
528         analyze(read)
529
530 for read in saved_reads: # second pass
531     if coverage(read, graph) >= DESIRED:
532         analyze(read)
```

533 Here, the space used for the graph remains identical to the digital normal-  
 534 ization algorithm and is typically sublinear in space for high coverage data  
 535 sets, but the algorithm is no longer single-pass, and requires re-examining  
 536 some subset of the input data in a second pass. In the worst case scenario,  
 537 with an undersampled source text (or randomly generated sentences), this  
 538 is a fully offline two-pass approach that requires re-examining *all* of the  
 539 input data for the second pass. In practice, most real data sets will require  
 540 fewer than two passes: graphically, any deviation from the identity line in  
 541 a saturation analysis as in Figure 4 yields a few-pass algorithm.

542 **Reduction to a streaming algorithm:** The semi-streaming algo-  
 543 rithm can be turned into a purely streaming algorithm in several special  
 544 cases - specifically, whenever reads need not be saved for a second pass.  
 545 One example is given above, in determining the error profile of sequencing  
 546 reads: here the error profile can be determined from only a small portion  
 547 of the data.

548 Another example of a purely streaming approach is when some portion  
 549 of correct data can be discarded, e.g. because of oversampling. (One  
 550 biological application for this occurs when the data set generated is large  
 551 enough to guarantee very high coverage of the entire genome.) In this  
 552 case, rather than saving reads for a second pass, only saturated reads are  
 553 analyzed, while reads that are not from saturated regions in the graph  
 554 are simply discarded. Applying this approach to the *E. coli* data set  
 555 used above, approximately 1/3 of the reads would be discarded while the  
 556 remaining 2/3 would be analyzed (see “Number of passes”, Table 11).

**Summary:** A summary of the three approaches developed above is presented in Figure 7. The two-pass approach in Figure 7(a) yields more efficient memory use, but with no advantage in execution time. The few-pass approach (Figure 7(b) combines the lower memory use with fewer passes across the data, and becomes more efficient as the coverage of the data set grows. Finally, the fully streaming approach in Figure 7(c) enables one-pass (or less) approaches for certain problems.

## 4 Discussion

### 4.1 Digital normalization can be applied effectively to short reads prior to error detection and correction.

Tracking k-mer abundances in large short-read data sets is part of many error detection and correction algorithms, but this process can be time and memory intensive. Here we show that for some data sets and several analyses, digital normalization can be used to reduce the total number of k-mers under consideration without strongly affecting results.

For example, with a real *E. coli* data set, digital normalization reduced the number of k-mers by a third (Table 3, Distinct k-mers) while spectral error prediction yielded essentially the same sensitivity and specificity of error predictions (compare columns in Table 3). Moreover, when we ran the Quake error corrector on the reads using unnormalized and normalized counts (Table 4), we achieved nearly identical results, demonstrating that the digitally normalized data set retained all of the information necessary for error correction.

### 4.2 K-mer counts from digitally normalized reads can be used to error correct mRNAseq data

Spectral error correction approaches typically rely on assumptions of uniform sequence coverage, but these assumptions are violated by several types of data, including mRNAseq and shotgun metagenome data. Digital normalization can be used to generate k-mer spectra with even coverage, allowing existing spectral error analysis approaches to be applied to data from samples with non-uniform abundances. We demonstrated this by using spectral error detection with digitally normalized data to predict errors in both synthetic and real RNAseq and metagenome data (Tables 7 and 8). We then again used Quake to error correct high-coverage portions of an mRNAseq data set, which yielded promising results (Table 9), although we note that the unusually high per-position error rate in this data may have led to poor results (Figure 6).

This again demonstrates that digitally normalized data retains the information necessary to error correct high coverage reads, despite having many fewer k-mers and total reads (Table 5 and Table 6). Note that we used the Quake software because it provided the option of using k-mer counts separate from the reads under analysis. While improved error

correction algorithms exist and could be evaluated with some modification, we believe the best path forward is to integrate the semi-streaming approach into an error corrector (below).

### 4.3 Short-read error detection can be done efficiently with a streaming few-pass sublinear-memory algorithm

K-mer spectral error detection, trimming, and correction approaches are typically implemented as a two-pass offline algorithm, in which k-mer counts are collected in a first pass and then reads are corrected in a second pass. While several algorithms that run in sublinear memory do exist (e.g., Lighter [8]), these are still offline algorithms that require two or more passes across the data.

In high coverage data sets it is possible to implement a more algorithmically efficient approach, by detecting reads that are high coverage in the context of reads previously encountered in the same pass of the data. We implemented this by integrating k-mer spectral error analysis directly into the digital normalization algorithm, and showed that on several synthetic and real data sets, we achieved nearly identical predictions to the full two-pass algorithm with an algorithm that is less than two pass (compare Table 8 to Table 11).

This near-equivalence of results is somewhat surprising, in that we appear to be able to reduce a two-pass offline algorithm to a semi-streaming approach requiring sublinear memory and fewer than two passes with little alteration of results. While data set characteristics affect the algorithmic performance (see “Time and space considerations”, above), the algorithm performs *more efficiently* with *more* data – a good trend.

As with digital normalization, a basic semi-streaming approach is very simple to implement: with an online way to count k-mers, the algorithm is approximately 10 lines of Python code. The approach also requires very few parameter choices: the only two parameters are k-mer size and target coverage. However, we do not yet know how these parameters interact with read length, error rate, or data set coverage; systematic evaluation of parameters and the development of underlying theory is left for future work. In practice, we expect that additional work will need to be done to adapt existing error correction approaches to use the semi-streaming approach.

### 4.4 Error trimming can be done efficiently with a semi-streaming algorithm

We next adapted the error detection algorithm to do semi-streaming error trimming on genomic, metagenomic, and transcriptomic data. On high coverage components of variable coverage data sets, this led to a substantial decrease in errors - up to an order of magnitude (Table 12).

The implementation of semi-streaming error trimming used in this paper is somewhat inefficient, and relies on redundantly storing all of the reads needed for the second pass on disk during the first pass. In the worst

case, where all reads are low coverage, a complete copy of the data set may need to be stored on disk! This is an area for future improvement. However, when we look at full data sets, fewer than half the reads are examined twice (see Number of passes, Table 13).

## 4.5 Data-set wide error profiles can be calculated in sublinear time and memory

The ability to analyze high-coverage reads without examining the entire data set offers some intriguing possibilities. One concrete application that we demonstrate here is the use of high coverage reads to infer data-set wide error characteristics for shotgun data, in a way that is robust to the sample type [26]. This approach could also be integrated directly into sequencers to assess whether the target coverage has been obtained, and perhaps stop sequencing. More generally, the approach of using saturating coverage to truncate computational analysis may have application to streaming sequencing technologies such as SMRT and Nanopore sequencing, where realtime feedback between sequencing and sequence analysis could be useful [29, 30].

## 4.6 Worst-case and best-case scenarios: when is error trimming best applied?

Here we introduce an approach to removing erroneous k-mers from large sequencing data sets with a semi-streaming algorithm that can be used on variable coverage data sets. When should this be applied?

The general semi-streaming algorithm is most time-efficient on data sets where much of the data is high coverage, because the second pass across the data is limited to the set of reads that is low coverage on the first pass (Figure 3). Even though the coverage of the data sets may not be known in advance, the approach is robust to low-coverage data: low-coverage reads can simply be ignored.

One particularly appealing aspect of the variable coverage error trimming approach is that it does not need to be modified for different data sets: the underlying algorithm can be applied equally to genomic, mRNAseq, and metagenome data sets, although read lengths, error rates, and data set coverage will affect the quality of results. On high coverage genomic data sets, trimming can be made more stringent by eliminating all low-abundance k-mers as erroneous, but even if this is not done, the underlying approach is equally efficient.

Digital normalization was developed primarily to decrease the memory requirements for De Bruijn graph assembly by eliminating erroneous k-mers; diginorm can reduce the memory requirements for Velvet by more than an order of magnitude [9]. However, diginorm also alters the coverage of the data set, which may affect the performance of assemblers or other downstream analysis steps that rely on coverage. While semi-streaming error trimming removes at least as many k-mers as digital normalization (and generally should remove many more), k-mer based error trimming should have a much smaller and far less biasing effect on data set coverage.



Moreover, trimming eliminates fewer reads than digital normalization. This may make trimming a more palatable pre-filter for assembly than digital normalization.

We caution against using variable coverage error trimming before mapping-based abundance analyses such as transcript quantification, ChIP-seq, or variant calling. Variable coverage error trimming preferentially retains low-abundance reads and eliminates portions of high abundance reads, which may bias results.

## 4.7 Conclusions

We describe a time- and memory- efficient algorithmic approach to k-mer spectral error detection and read trimming based on read-local analysis of coverage. This approach can be applied generically to variable coverage data, including mRNAseq and shotgun metagenome reads. Moreover, the approach should be straightforward to integrate into existing k-mer based spectral analyses, including error correction and assembly pipelines. Future applications could include semi-streaming error correction, reference-free variant calling, and reference-free analysis of streaming sequencing data.

## References

- [1] Pevzner PA, Tang H, Waterman MS (2001) An eulerian path approach to dna fragment assembly. *Proc Natl Acad Sci U S A* 98: 9748-53.
- [2] Kelley DR, Schatz MC, Salzberg SL (2010) Quake: quality-aware detection and correction of sequencing errors. *Genome Biol* 11: R116.
- [3] Zhang Q, Pell J, Canino-Koning R, Howe AC, Brown CT (2014) These are not the k-mers you are looking for: efficient online k-mer counting using a probabilistic data structure. *PLoS ONE* 7.
- [4] Charikar M (2004) Finding frequent items in data streams. *Theoretical Computer Science* 312: 3–15.
- [5] Cormode G, Muthukrishnan S (2005) An improved data stream summary: the count-min sketch and its applications. *Journal of Algorithms* 55: 58–75.
- [6] Feigenbaum J, Kannan S, McGregor A, Suri S, Zhang J (2005) On graph problems in a semi-streaming model. *Theor Comput Sci* 348: 207–216.
- [7] Melsted P, Halldorsson BV (2014) KmerStream: streaming algorithms for k-mer abundance estimation. *Bioinformatics* 30: 3541–3547.
- [8] Song L, Florea L, Langmead B (2014) Lighter: fast and memory-efficient sequencing error correction without counting. *Genome Biol* 15: 509.

- [9] Brown CT, Howe A, Zhang Q, Pyrkosz AB, Brom TH (2012) A reference-free algorithm for computational normalization of shotgun sequencing data. *arXiv* : 1203.4802.
- [10] Chitsaz H, Yee-Greenbaum JL, Tesler G, Lombardo MJ, Dupont CL, et al. (2011) Efficient de novo assembly of single-cell bacterial genomes from short-read data sets. *Nat Biotechnol* 29: 915–921.
- [11] Grabherr MG, Haas BJ, Yassour M, Levin JZ, Thompson DA, et al. (2011) Full-length transcriptome assembly from RNA-Seq data without a reference genome. *Nat Biotechnol* 29: 644–652.
- [12] Shakya M, Quince C, Campbell JH, Yang ZK, Schadt CW, et al. (2013) Comparative metagenomic and rRNA microbial diversity characterization using archaeal and bacterial synthetic communities. *Environ Microbiol* 15: 1882–1899.
- [13] Flajolet P, Fusy É, Gandouet O, Meunier F (2008) Hyperloglog: the analysis of a near-optimal cardinality estimation algorithm. *DMTCS Proceedings* .
- [14] Lowe EK, Swalla B, Brown C (2014) Evaluating a lightweight transcriptome assembly pipeline on two closely related ascidian species. *PeerJ Preprints* 2.
- [15] Marcais G, Kingsford C (2011) A fast, lock-free approach for efficient parallel counting of occurrences of k-mers. *Bioinformatics* 27: 764–770.
- [16] Schäling B (2011) The boost C++ libraries. Boris Schäling.
- [17] Langmead B, Salzberg SL (2012) Fast gapped-read alignment with Bowtie 2. *Nat Methods* 9: 357–359.
- [18] Chitsaz H, Yee-Greenbaum J, Tesler G, Lombardo M, Dupont C, et al. (2011) Efficient de novo assembly of single-cell bacterial genomes from short-read data sets. *Nat Biotechnol* 29: 915–21.
- [19] Roberts A, Pachter L (2011) RNA-Seq and find: entering the RNA deep field. *Genome Med* 3: 74.
- [20] Medvedev P, Scott E, Kakaradov B, Pevzner P (2011) Error correction of high-throughput sequencing datasets with non-uniform coverage. *Bioinformatics* 27: i137–41.
- [21] Le HS, Schulz MH, McCauley BM, Hinman VF, Bar-Joseph Z (2013) Probabilistic error correction for RNA sequencing. *Nucleic Acids Res* 41: e109.
- [22] Qu W, Hashimoto S, Morishita S (2009) Efficient frequency-based de novo short-read clustering for error trimming in next-generation sequencing. *Genome Res* 19: 1309–1315.
- [23] Howe AC, Jansson JK, Malfatti SA, Tringe SG, Tiedje JM, et al. (2014) Tackling soil diversity with the assembly of large, complex metagenomes. *Proc Natl Acad Sci U S A* 111: 4904–9.
- [24] Haas BJ, Papanicolaou A, Yassour M, Grabherr M, Blood PD, et al. (2013) De novo transcript sequence reconstruction from rna-seq using the trinity platform for reference generation and analysis. *Nat Protoc* 8: 1494–512.

777 [25] Lander ES, Waterman MS (1988) Genomic mapping by fingerprinting  
778 random clones: a mathematical analysis. *Genomics* 2: 231–239.

779 [26] Keegan KP, Trimble WL, Wilkening J, Wilke A, Harrison T,  
780 et al. (2012) A platform-independent method for detecting errors  
781 in metagenomic sequencing data: DRISSEE. *PLoS Comput Biol* 8:  
782 e1002541.

783 [27] Dohm JC, Lottaz C, Borodina T, Himmelbauer H (2008) Substan-  
784 tial biases in ultra-short read data sets from high-throughput DNA  
785 sequencing. *Nucleic Acids Res* 36: e105.

786 [28] Pell J, Hintze A, Canino-Koning R, Howe A, Tiedje JM, et al. (2012)  
787 Scaling metagenome sequence assembly with probabilistic de bruijn  
788 graphs. *Proc Natl Acad Sci U S A* 109: 13272–7.

789 [29] Eid J, Fehr A, Gray J, Luong K, Lyle J, et al. (2009) Real-time DNA  
790 sequencing from single polymerase molecules. *Science* 323: 133–138.

791 [30] Howorka S, Cheley S, Bayley H (2001) Sequence-specific detection of  
792 individual DNA strands using engineered nanopores. *Nat Biotechnol*  
793 19: 636–639.